I R A M P
3(1), June 2012, pp. 51-59

ISSN: 2229-3159

Analysis of TiO Spectral Transitions in Laser-induced and Radio-frequency Thermal Plasmas

**ALEXANDER C. WOODS[1], CHRISTIAN G. PARIGGER[1], ANNA KESZLER[2]
LÁSZLÓ NEMES[3], JAMES O. HORNKOHL[4]**

[1]The University of Tennessee, UT Space Institute, Center for Laser Applications, 411 B.H. Goethert Parkway Tullahoma, TN 37388-9700, USA
[2]Chemical Research Center of the Hungarian Academy of Sciences, Institute of Materials and Environmental Chemistry Puszataszeri ut 59-67, H-1025 Budapest, Hungary
[3]Chemical Research Center of the Hungarian Academy of Sciences, Laser Spectroscopy Laboratory Puszataszeri ut 59-67, H-1025 Budapest, Hungary
[4]Hornkohl Consulting, Tullahoma, TN 37388, USA

ABSTRACT: The spectral transitions of titanium monoxide (TiO), contained in stellar spectra for K-type and M-type stars, have long been observed by astronomers. Recent interest in the titania (TiO_2) nanoparticle for thin film fabrication brings additional interest in the analysis of the TiO molecular transitions in a plasma. The transition bands for the TiO molecule are numerous and often overlap one another on a spectral region. This research involves the calculation of predicted spectra for the TiO γ, γ', and E-X $\Delta v = 0$ transition bands. The synthetic spectra are then used to infer temperature. This is accomplished through nonlinear fitting, using a Nelder-Mead algorithm, of the predicted spectra with collected spectra. In this work, spectra are obtained by two distinct methods. In one experiment, a radio-frequency (RF) thermal plasma reactor is utilized, while the other experiment collects spectra following laser-induced optical breakdown (LIB).

PACS:52.50.Jm, 52.25.Os, 32.70.Fw, 32.30.-r, 33.20.-t, 81.15.Fg

Keywords: Laser Plasma, Line Strengths, Atomic and Molecular Spectra, Laser Ablation, Film Deposition

1. INTRODUCTION

The experimental procedure for this research was performed at the Chemical Research Center of the Hungarian Academy of Sciences (CHEMRES) and the University of Tennessee Space Institute (UTSI). This communication expounds on initial investigations reported at the International High-Power Laser Ablation conference[1]. Here, previously presented data resulting from the radio-frequency thermal plasma investigations of the TiO A-X, γ, band has been sensitivity corrected and the B-X, γ', band is examined in more detail on a narrower wavelength range. Also, the TiO γ' band is analyzed at various time delays following laser-induced breakdown.

The several bands of TiO stretching from the visible to the near infrared have been historically significant in astronomy [2, 3]. These TiO bands are very prominent in the spectra of late type stars, especially considering the molecule's relatively low abundance within stars [4]. In fact, the TiO electronic band systems are so dominant in the visible spectrum of M-type stars that the band systems are the primary criterion in establishing the spectral type [5]. A great deal of work consisting of experimental investigations and theoretical development of the electronic transition band systems of TiO have been undertaken on account of the significance of the molecule in stellar observations. In examining late-K and early-M type dwarf stars, TiO bands have been analyzed to determine the amount of oxygen present in these stars [6], while the temperature sensitivity of molecular band intensities for diatomic molecules have provided a useful tool in determination of excitation temperatures [7, 8, 9].

In part due to its photocatalytic properties [10], TiO_2, is a very promising molecule for thin film applications. Among the various applications, TiO_2, may be used for purification and treatment of water and air[11], and it serves as a worthy candidate for use in solar cells [12, 13]. Generation of TiO_2, nanoparticles has historically been accomplished by use of a RF thermal plasma[14] or by pulsed laser deposition (PLD)[15]. In the development of both RF plasma and pulsed laser deposition techniques concerning titanium, it is of interest to know the temperature of TiO in the ablation plume [16, 17], since in these cases TiO is a precursor to the longer lived TiO_2 molecule. The method of laser-induced breakdown spectroscopy (LIBS) provides a valuable tool for experimental analysis. The procedure provides a reliable way of determining micro-plasma parameters [18]. This is accomplished by first collecting spectra following laser-induced breakdown (LIB). The collected spectra is then compared to predicted spectra computed for the diatomic molecule of interest with varying micro-plasma parameters[19]. In this case, the comparison is made by fitting the measured spectra with calculated spectra by use of a Nelder-Mead or amoeba algorithm [20]. The Nelder-Mead method allows for a multi-parameter fit, from which the micro-plasma parameters are inferred.

2. THEORETICAL APPROACH

In calculating predicted spectra for diatomic molecules, a quantity know as the line-strength is of great importance. A line-strength, S_{ul}, may be defined as

$$S_{ul} = \sum_u \sum_l |\langle u | T_\kappa^{(q)} | l \rangle|^2 . \tag{1}$$

The summations account for all upper (u) and lower (l) states that produce that particular spectral line, while $T_\kappa^{(q)}$ is the κ^{th} component of the irreducible tensor of order q responsible for the transition. Quantities like the Einstein coefficients, oscillator strength, and cross section are very familiar. However, the line strength is significant because it is the term in which some of the more familiar terms are defined [21, 22]. The Einstein A coefficient, for example, may be written

$$A_{ul} = \frac{2\omega_{ul}^3}{3\varepsilon_0 h c^3 g_u} S_{ul} . \tag{2}$$

Here, ω_{ul} is the transition frequency ($\omega_{ul} = 2\pi\nu_{ul}$), ε_0 is the vacuum permittivity, h is Planck's constant, c is the speed of light, and g_u is the upper level degeneracy.

Computed spectra consists of line-strength files. These line-strengths are defined by the unitless Hönl-London factors,

$$S(J',J) = \frac{1}{2J+1} \left| \sum_{a'} \sum_{a} \langle nvJM \,|\, a \rangle \langle J\Omega q\kappa \,|\, J'\Omega' \rangle \langle a' \,|\, n'v'J'M' \rangle \right|^2 \delta_{S'S} \delta_{\Sigma'\Sigma} , \tag{3}$$

and the electronic-vibration strength,

$$S(n'v', nv) = \sum_{\kappa=-q}^{q} \left| \langle nv \,|\, \hat{T}_\kappa^{(q)} \,|\, n'v' \rangle \right|^2 , \tag{4}$$

which has units of line-strength. In the above equation providing the Hönl-London factors, ν represents the vibrational quantum number, J the total angular momentum, M the magnetic quantum number for the laboratory z-component of the total angular momentum, Ω is for the z′-component of the total angular momentum, S the spin, Σ the spin for the z′-component, a represents the Hund's case a basis, and n represents all other necessary quantum numbers. The Hönl-London factors provide a measure of the allowable angular momentum transitions. In some cases, the Hönl-London factors are equal to zero. Therefore, the Hönl-London factors may be used as a selection rule [23].

Now, the electronic-vibrational strength, $S(n'v', nv)$, consists of the electronic transition moment. To compute this, it becomes necessary to separate the electronic and nuclear vibrational and rotational elements. In other words, we make the Born-Oppenheimer approximation,

$$\langle n'v' | \hat{T}_{\kappa}^{(q)} | nv \rangle \approx \langle n' | \hat{T}_{\kappa}^{q} | n \rangle \langle v' | v \rangle = \mathsf{R}_{n'n}(r) \langle v' | v \rangle. \tag{5}$$

This allows for the electronic transition moment, $\mathsf{R}_{n'n}(r)$, to become separated from the overlap integral, $\langle v' | v \rangle$. In order to analytically calculate the electronic-vibrational strength for each allowed transition, the electronic transition moment is expanded using a Taylor's series,

$$\mathsf{R}_{n'n}(r) = a_0 + a_1 r + a_2 r^2 + \ldots \tag{6}$$

Finding the Franck-Condon factors for the vibrational transitions,

$$q(v', v) = \langle v' | v \rangle^2 = \left| \int_0^{\infty} \psi_{v'}(r)\, \psi_v(r)\, dr \right|^2, \tag{7}$$

and computing r-centroids representing the distance between the two nuclei,

$$\bar{r}^{(k)}(v', v) = \frac{\langle v' | r^k | v \rangle}{\langle v' | v \rangle} = \int_0^{\infty} \psi_{v'}(r)\, r^k\, \psi_v(r)\, dr \;\Big/ \int_0^{\infty} \psi_{v'}(r)\, \psi_v(r)\, dr. \tag{8}$$

The electronic-vibrational strength becomes

$$S(n'v', nv) = \left[a_0 + a_1 \bar{r}^{(1)}(v', v) + a_2 \bar{r}^{(2)}(v', v) \ldots \right]^2 q(v', v). \tag{9}$$

The initial focus of this research has been placed on the TiO γ, γ′, and E-X 0-0 transition systems. These band systems have been chosen due to the availability of tabulated angular momentum transition values, which were experimentally obtained. A computer program was then implemented, calculating the upper and lower Hamiltonian matrix values. The resulting Franck-Condon factors are explicitly given in [1]. This allows for the generation of line-strength files, which may be plotted for various temperatures and spectroscopic parameters. Accurate spectrum predictions require, at least, a temperature for Boltzmann factors and may also include spectral resolution, electron density, reaction rates, collision rates, and pressure.

The TiO molecule has many band systems, and these band systems overlap one another across the TiO spectrum. This presents a greater challenge in properly identifying and characterizing the TiO molecule in a micro-plasma. This is because at regions of overlap, multiple transitions must be superposed and fit to obtain accurate inference of parameters of interest. However, accomplishing this may provide information on relative prominence of specific transitions occurring. As a result of the abundance of TiO transition bands and their overlapping, more computational work is necessary to fully understand the TiO spectrum.

3. EXPERIMENTAL TECHNIQUE

The experiments performed were aimed at identifying and characterizing the TiO γ and γ′ systems. This was accomplished by a collaboration between the Chemical Research Center of the Hungarian Academy of Sciences (CHEMRES) and the University of Tennessee Space Institute (UTSI). The experiment at the Chemical Research Center of the Hungarian Academy of Sciences consisted of feeding TiO_2, powder into a radio-frequency (RF) plasma reactor, while those at the University of Tennessee Space Institute involved the focusing of nanosecond pulsed laser excitation onto a solid titanium sample.

3.1. RF Thermal Plasma Spectroscopy

Figure 1 illustrates the experimental arrangement for thermal plasma spectroscopy. The thermal plasma technique involved a water-cooled plasma reactor, cyclone, filter unit, and a vacuum pump. The radio-frequency plasma

reactor utilized a PRAXAIR powder feeder to axially inject the TiO_2 through a water-cooled probe into the microwave plasma. A TEKNA PL-35 torch was used to excite the plasma. Here, the TEKNA PL-35 is inductively coupled to a plate power of 20-30 kW. A generator operating at 3-5 MHz provides the RF power.

The plasma emissions are observed through a quartz glass window. At a distance of 0.1 m from the bottom of the plasma nozzle, the window provides a view perpendicular to the axis of the microwave plasma. These emissions are channeled through a fiber optic bundle to be dispersed by a TRIAX 550 Jobin-Yvon 0.55 m focal length monochromator. This provides a reciprocal dispersion of 1.55 nm/mm by employing a 1200 grooves/mm grating. The radiation is then detected and recorded by a CCD-3000 optical multi-channel analyzer.

The measured spectra from the RF thermal plasma contains a great deal of structure. In the region where γ' is expected to be prominent, many other transitions may be identified. The TiO α and β systems [3, 24] are likely contributors based on the presence of their band heads in other parts of the measured spectra. Also, many Ti I lines are readily identified through out the spectra.

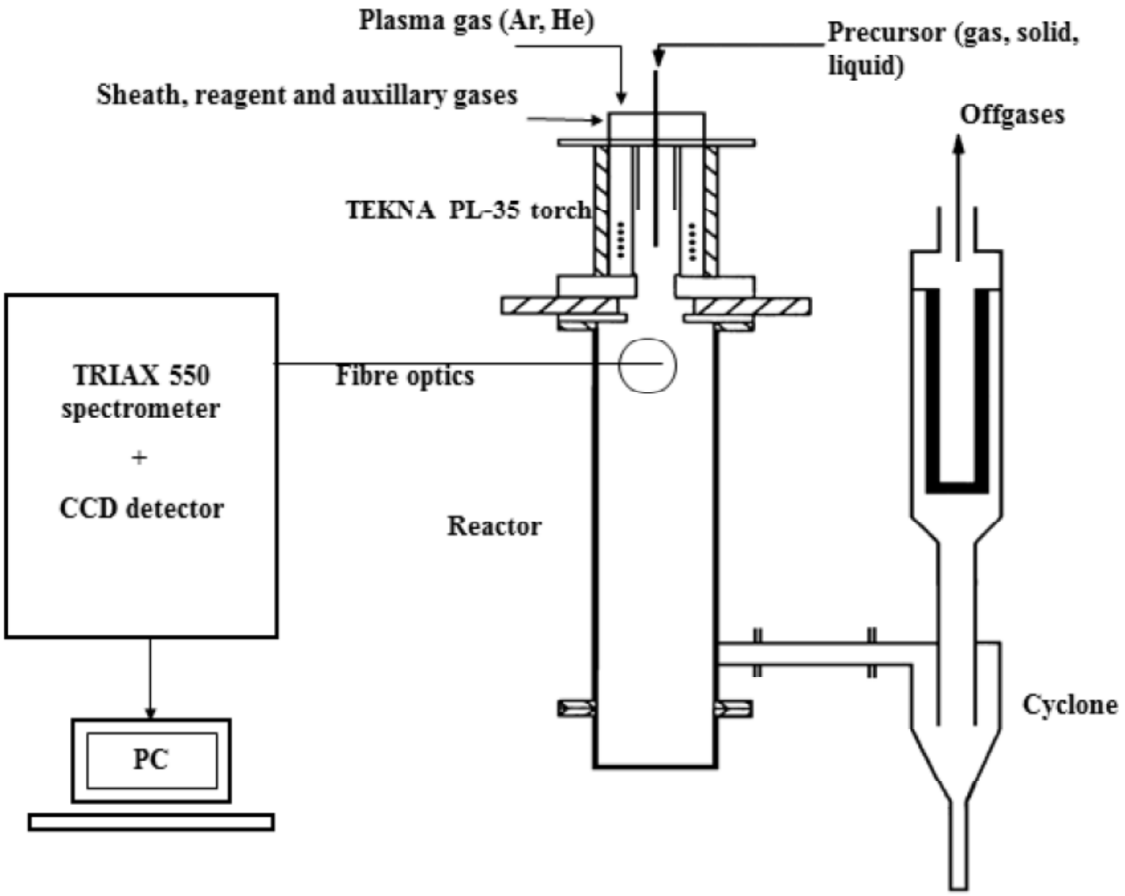

Figure 1: Experimental schematic of thermal plasma experiment

By examining the spectral range of collected spectra, the A-X and B-X TiO molecular transitions are clearly prominent. After the measured spectra [1] are wavelength-sensitivity corrected, it is then fit with synthetic spectra calculated for a full-width half maximum (FWHM) spectral resolution of 0.05 nm. For the γ system, a temperature of $T = 2903\ K$ is inferred. Figure 2 illustrates the results. Similarly, at the same spectral resolution a temperature of $T = 4423$ K may be inferred for the TiO γ' system. Figure 3 shows the measured and fitted spectra. The one-sigma error margins for temperature inferred from AX and BX are on the order of 2% to 4% and 15% to 20%, respectively [1].

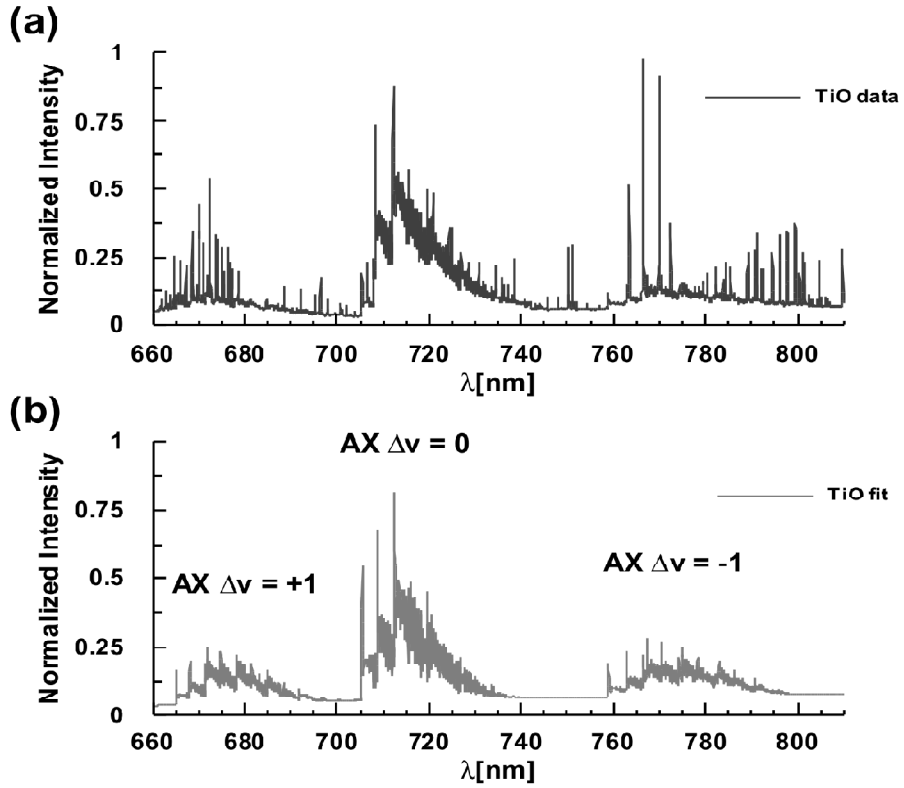

Figure 2: (a) Collected and (b) fitted spectra representing the γ A-X Δ*v* = -1,0,+1 systems. The inferred temperature amounts to T = 2903 K

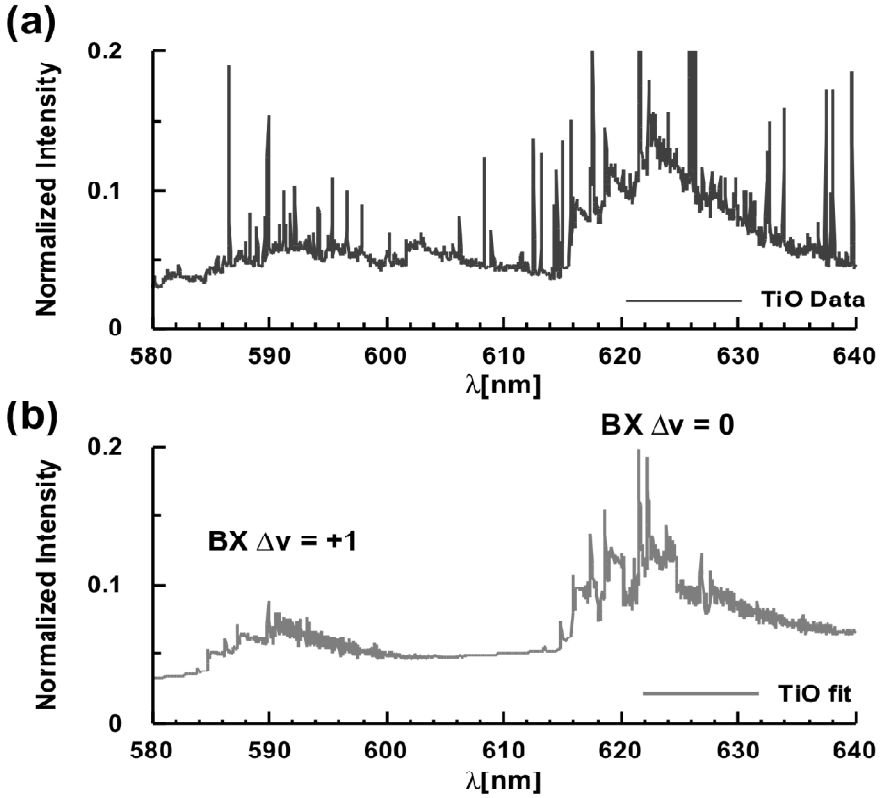

Figure 3:(a) Collected and (b) fitted spectra representing the γ′, B-X Δ*v* = 0,+1 systems. The inferred temperature amounts to T = 4423 K

3.2. Laser-induced Breakdown Spectroscopy

An important aspect of measuring molecular spectra in a laser-induced plasma is choice of time delay from laser-plasma generation. Molecular structure only becomes discernable on the order of microseconds after optical breakdown. In order to make measurements of the TiO spectra in the laser-induced micro-plasma at various time delays, the laser as well as the spectrometer must be synchronized accordingly. Here, this goal is initialized by a Wavetek FG3C wave generator. Figure 4 shows the experimental arrangement. The signal is sent to an optical multichannel analyzer (OMA) synchronization box. The synchronization box then sends the signal to event and sync inputs on an OMA EG&G. The synchronization box also sends a signal from another output to the delay generator. The delay generator, now triggered by the wave generator, then relays the signal to trigger our laser's flash lamp. Another output of this delay generator is then sent to the back of the OMA EG&G. The OMA is now synchronized with the synchronization box. This setup allows for control of when the OMA begins reading data by adjusting a delay on the delay generator.

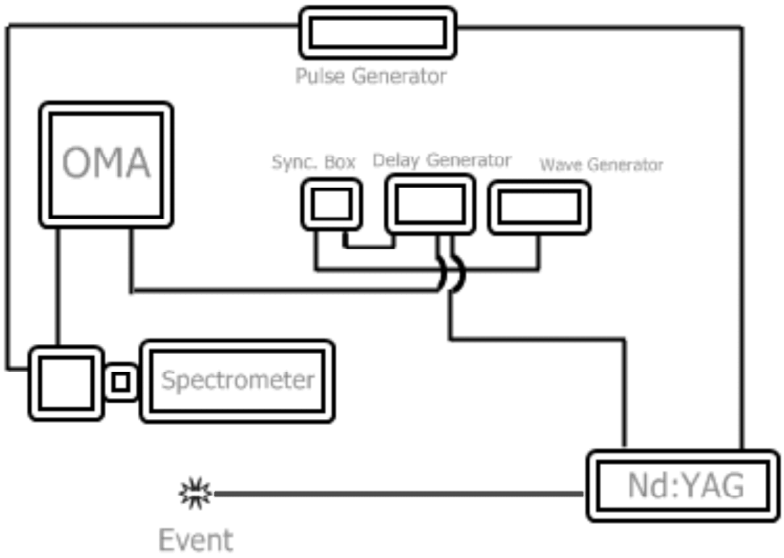

Figure 4: Experimental schematic of the LIBS experiment

The setup also consisted of a 0.5m model 500 SpectraPro Acton Research Corporation spectrometer and an intensified linear diode array (model 1460 Princeton Applied Research detector/controller optical multichannel analyzer), as the spectrometer and detector. For the excitation source, a 13 ns Q-switched Nd:YAG Quanta-Ray DCR-2A(10) laser operating at its fundamental wavelength of 1064 nm with 90 mJ per pulse was used. The 1064 nm wavelength was focused vertically downward on the flat surface of a titanium sample, while the 532 nm wavelength portion of the beam was deflected to a beam stop. In order to reduce the effects of craters from previous laser ablation, the titanium sample was rotated as data was collected.

For satisfactory measurements, the spectrometer and optical multichannel analyzer were wavelength calibrated by use of a hydrogen lamp to locate the H Balmer series peak. The equipment was also intensity calibrated. This was accomplished by using a Leeds and Northrup Co. optical pyrometer to measure the temperature of an active tungsten lamp. A blackbody curve was then calculated for the corresponding temperature, and the measured spectral intensity of the lamp was compared to the curve for each wavelength range measured. This provided an intensity calibration factor for each pixel corresponding to every wavelength measured. These calibration factors were then applied to the collected spectra.

The observed spectra from the ablation plume above the metal sample contain a significant amount of background. Here, background refers to any spectral contribution other than the specific transition band of interest. This background consists of other TiO molecular transitions, Ti atomic transition lines, along with likely molecular and atomic contributions from the laboratory air. In order to aid the characterization of the diatomic molecular structures

observed, a Savitzky-Golay filter [25] was applied to the data set. Figure 5 displays the typical action of this filter. This particular filter diminishes high-frequency components/noise, but may affect spectroscopic appearance of narrow peaks. We find in our analysis of the TiO bands that the inferred temperature is not affected within the one-sigma error margin. Fig. 5 also shows the difference of measured and filtered data. Clearly, near the narrow peaks on the order of at most 10% may be lost to the action of the filter.

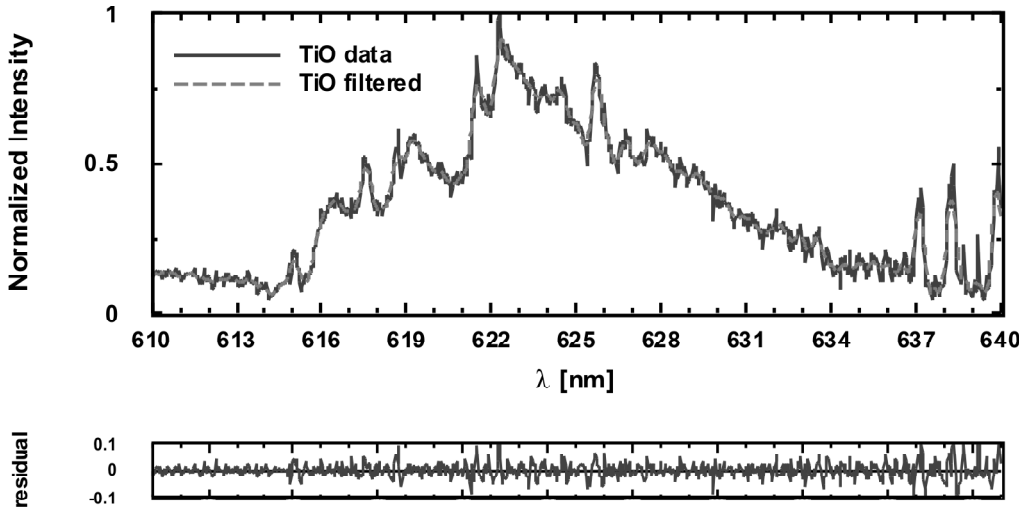

Figure 5: Savitzky-Golay filter application to single shot spectra. The inset shows the residual of measured and filtered data

Since the LIBS technique allows for time-resolved spectroscopic measurements, the transition bands were measured at varying delay times following LIB. Figure 6 displays the observed spectra 52 μs and 72 μs after LIB, and it shows the synthetic spectra corresponding to the inferred temperature of T = 3591 K and T = 4141 K, respectively. The Savitzky-Golay filter was comprised of 31-point, 6-th order polynomial. The one-sigma error margin for this analysis is similar to previous analysis of unfiltered data, and is on the order of 15% to 20% [1]. Consequently, the inferred temperatures are not-significantly different for the measured spectra at the two time delays of τ = 52 μs and τ = 72 μs from LIB. However, comparison of Fig. 6 (a) and (b) reveals differences in appearance of atomic lines near 618-nm and 628-nm. Studies of the Ti atomic lines are contents of ongoing spectral analysis in the region of TiO AX and BX bands.

4. DISCUSSION

Our calculations provide spectral predictions of the bands from 599-945 nm, the bands from 582-679 nm, and the E-X 0-0 at 836-857 nm. For RF thermal plasma experiment, a spectral range of 200-1000 nm is achieved. Thus, this setup provided a wide-range view of the numerous observable TiO transitions. By inspecting the spectra collected from this approach, several transition bands, which we do not have predicted spectra for, may be identified by comparison with previous published works. Examples include indications of blue-green bands [3] and the α band 566.1 nm (0-2)[24]. The spectra also reveal a great deal of atomic Ti lines.

For the LIBS experiment, the measurements focus on wavelengths from 555-640 nm. Interestingly, the inferred temperatures for the transitions seen in Fig. 6 report a higher TiO temperature at the later time delay. This might be characteristic of the evolution of TiO in the laser-induced plasma. However, it must be noted that Monte-Carlo simulations utilizing 25% background variation for similar data may produce error bars for the inferred temperatures on the order of several hundred degrees Kelvin[1].

On the wavelength interval of 580-610 nm, our measurements indicate the presence of two different TiO transition band profiles. While both are present in the measured spectra, matching of the computed spectra of each band system maintains minimal overlap in the region. In principle, the relative intensities of the two systems may be used to determine the relative prominence in the plasma.

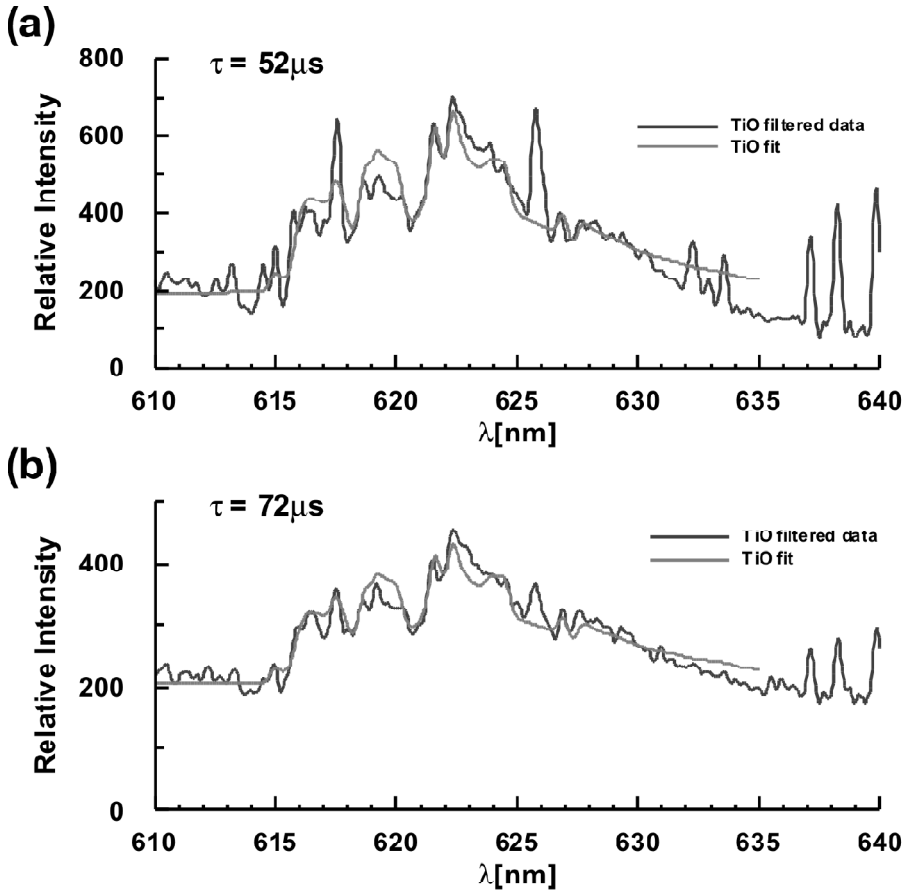

Figure 6: (a) t = 52 μs and (b) t = 72 μs measured and fitted spectra representing the system at T = 3591 and T = 4141 K, respectively

However, through much of the collected spectra there appears to be quite a bit of overlapping of transition bands. By examining Fig. 2 and Fig. 3 for the RF thermal plasma and Fig. 5 and Fig. 6 for the laser-induced plasma, one will notice significant background contributions. While the atomic lines may be readily identified, the presence of multiple TiO transitions along with potentially other diatomic molecular transitions contribute to the prominent background observed.These background contributions are also present in the sensitivity corrected band measurement displayed in Fig. 2, over and above presenced a volley of titanium atomic lines.

Currently, our Nelder-Mead fitting method is designed to fit one transition band at a time. The presence of multiple transition bands and atomic lines in measured spectra contribute to what is considered the background to the transition band being fitted.The background observed in these measurements is determined to have the effect of raising the inferred temperature. Since much of the measured spectra contain significant overlapping of the TiO molecular transitions along with atomic lines for Ti and other species in our laboratory air, there remains much work left undone.

In order to aid the fitting routine, a Savitzky-Golay filter is applied to the measured spectra. The Savitzky-Golay filter provides a method for smoothing the collected data. This effectively removes the higher frequency oscillations, which is often termed as noise. By employing this technique, the most prominent transition structure is revealed. However this structure, which represents the transitions of interest, will be smoothed as well. The difference spectrum between the collected spectra and the smoothed spectra, illustrated at the bottom of Fig. 5, indicates several peak values. These peak values show the loss of distinct structure to the filter, which may affect the inferred temperature. In this experiment, the effect results in temperature variations well within the indicated one-sigma error margin.

Two of us (ACW and CGP) thank for support in part by the Center for Laser Applications at the University of Tennessee Space Institute.

References

[1] C. G. Parigger, A. C. Woods, A. Keszler, L. Nemes, and J. O. Hornkohl, High Power Laser Ablation Conference Proceedings, Santa Fe, NM, May 2012.

[2] K. C. Namiki, H. Saitoh, and H. Ito, *J. Mol. Spectrosc.*, **226**, 87-94, (2004).

[3] A. Christy, *Phys. Rev.* **33**, 701-730, (1929).

[4] H. G. Jorgensen, Astron. *Astrophys.* **284**, 179-186, (1994).

[5] D. Kotnik-Karuza and R. Jurdana-Sepic, Astron. *Astrophys.* **355**, 595-602, (2000).

[6] S. J. Schmidt, G. Wallerstein, V. Woolf, and J. L. Bean, AIP 978-0-7354-0627-8, (2009).

[7] J. G. Phillips, *ApJ* **119**, 274-285, (1954).

[8] A. Milone and B. Barbuy, Astron. *Astrophys. Suppl.* **108**, 449-454, (1994).

[9] J. A. Valenti, N.E. Piskunov, and C. M. Johns-Krull, *ApJ* **498**, 851-862, (1998).

[10] A. L. Linsebigler, G. Lu, and J. T. Jr. Yates, *Chem. Rev.* **95**, 735, (1995).

[11] D. F. Ollis, C. R. Acad. Sci. Ser. IIC **3** (6), 405-411, (2000).

[12] B. O'Regan, M. Grätzel, *Nature* **353**, 737, (1991).

[13] C. D. Grant, A. M. Schwartzberg, G. P. Smestad, J. Kowalik, L. M. Tolbert, and J. Z. Zhang, *J. Electrochem. Soc.* **522**, (1), 40-48, (2002).

[14] J-G Li, H. Kamiyama, X. H. Wang, Y Moriyoshi, and T. Ishigaki *J. Eur. Ceram. Soc.* **26**, 423-428, (2006).

[15] S. Yamamoto, T. Sumita, A. Miyashita, and H. Naramoto, *Thin Solid Films*, **401**, 88-93, (2001).

[16] J-G Li, M. Ikeda, R. Ye, Y. Moriyoshi, and T. Ishigaki, *J. Phys. D: Appl. Phys.* **40**, 2348-2353, (2007).

[17] J. Hermann, A. Peronne, and C. Dutouquet, *J. Phys. B: At. Mol. Opt. Phys.* **34**, 153-164, (2001).

[18] C. G. Parigger and E. Oks, *Int. Rev. Atom. Mol. Phys.* **1**, 13-23, (2010).

[19] C. G. Parigger and J. O. Hornkohl, *Int. Rev. Atom. Mol. Phys.* **1**, 25-43, (2010).

[20] I. G. Dors, C. Parigger, and J. W. L. Lewis, *Opt. Lett.* **23**, 1778-1780, (1998).

[21] R. C. Hilborn (1981), Am. J. Phys. **50**, 982-986, Erratum 51, 471 (1982), revision available at *http://arxiv.org/abs/physics/0202029* (2002).

[22] J. O. Hornkohl, L. Nemes, and C. G. Parigger, "Spectroscopy of Carbon Containing Diatomic Molecules," in: L. Nemes, S. Irle (Eds.), *Spectroscopy, Dynamics and Molecular Theory of Carbon Plasmas and Vapor*, (World Scientific, Singapore, 2011), 113-165 (2011).

[23] C. G. Parigger and J. O. Hornkohl, Spectrochim. Acta, Part A, **81**, (1), 404-411, (2011).

[24] C. M. Pathak, and H. B. Palmer, *J. Molec. Spectrosc.* **33**, 137-146, (1970).

[25] W. H. Press, S. A. Teukolsky, W. T. Veterling, and B. P. Flannery, *Numerical Recipes, The Art of Scientific Computing*, 3rd edition, (Cambridge University Press, New York, 2007), 766-772, (2007).